Oberst and aging tests of damped CFRP materials: New Fitting procedure and experimental results

Oberst and aging tests of damped CFRP materials: new fitting procedure and experimental results

Alessandro Fasana[1], Alessandro Ferraris[3], Andrea Giancarlo Airale[4], Davide Berti Polato[5] and Massimiliana Carello[2]
[1]Politecnico di Torino, Italy, e-mail: alessandro.fasana@polito.it
[3]Politecnico di Torino, Italy, e-mail: alessandro.ferraris@polito.it
[4]Politecnico di Torino, Italy, e-mail: andrea.airale@polito.it
[5]Politecnico di Torino, Italy, e-mail: davide.bertipolato@polito.it
[2]Politecnico di Torino, Italy, e-mail: massimiliana.carello@polito.it

ABSTRACT
Materials play a fundamental role in defining the vibrational and acoustic characteristics of structures and their importance is even increasing because of the continuing demand for lightweight products. Carbon Fibre Reinforced Plastics (CRFP) components are becoming more and more popular because of their excellent mechanical properties but are unfortunately almost unable to dissipate energy. This is one of the reasons why their usage is limited to structural components and does not directly affect acoustic and vibrational response, which are among the factors responsible for harshness and comfort. In vehicles, for example, large panels of CFRP are as noisy as metallic panels so that this kind of lightweight structures is only used when a limited mass is of paramount importance, e.g. in racing cars. The chance of incorporating a damping material in the stacking sequence of CF layers that define a composite seems to be a viable solution to ameliorate the vibrational behavior of composite materials. This configuration permits to cure the damping layers together with the resins, in order to obtain both free and constrained layer solutions.
In this paper, the Oberst beam method has been chosen to determine the elastic modulus and loss factor of such materials, as a function of both frequency and temperature. Three nominally identical samples for each configuration have been tested in a temperature controlled environment, according to the Oberst beam test method. The effects of aging have been simulated by an accelerated standard procedure, with cyclically varying temperature and humidity for a total of 792 hours (3 cycles x 264h). The analysis of experimental data has been performed in the frequency domain by a least square fitting procedure, aimed at outperforming the simple half-power point method. An open source version of the fitting technique has also been implemented and can be obtained from the authors under the CC-by license.
.

KEYWORDS
Oberst test, aging, fitting, damping material, composite, carbon fiber reinforced plastics

1 INTRODUCTION

Lightweight design and noise reduction are two of the hot spots of vehicle manufacturers as explained in [1,2]. These two critical topics are treated in this article starting with the analysis of CFRP mechanical behaviour and continuing with the integration of rubber-based compound to obtain a lightweight damped composite. The proposed target is the integration of damping material between CFRP layers, maintaining as constant as possible the mechanical and weight characteristics of composite while improving the NVH property. Nowadays the integration of the damping material in the stacking sequence is performed in two ways:

- external application on the surfaces of produced components (free layer formulation);
- integration between layers of CFRP (constrained layer formulation).

A noticeable characteristic of damping material used in this research is the possibility of integration in the CFRP, before the cure procedure, whose effects can be analyzed in deep as performed by [3]. This characteristic is interesting because their application can be integrated into the production process maintaining under control the technology and final product costs.

Material characterization is performed using Oberst test standard (following [4]), avoiding the use of destructive test as in [5,6]. The use of non-destructive Oberst test, to define Young modulus and loss factor of damping and structural materials, is preferred because of its capability to test exactly the same specimens at different environmental conditions. The use of vibrational and non-destructive test permits the repeatability and the immediate evaluation of damping characteristics as in [7].

The effect of temperature and aging effect must be considered to verify if any unwanted damping decrement occurs, which could increase the vibration criticalities. In fact, the final use of these materials is on road vehicles where a vibration and noise increment gives the perception of quality decrement to the customer. For this reason, the aging tests have been integrated to the thermal Oberst tests taking under control the material performance degradation. Nowadays, the acoustic comfort is achieved by applying massive sound and vibration deadening materials on critical areas, such as the bonnet, door panel, roof and floor. Considering the new target of automotive weight reduction those solutions are not suitable for new applications, therefore innovative solutions and materials are analyzed in this article.

2 TEST METHODOLOGY

The aim of the study is the characterization of a CFRP sandwich, with and without a damping layer, at different temperatures, and also the documentation of its variations (if any) under an accelerated aging cycle. The damping material is basically a rubber based compound which can be produced in thin, flexible, large and light sheets. It can very simply be included in the stacking sequence of any CFRP component, beams in the present examples but also in more complicated structures, and can undergo the same curing process as the resins. These qualities make it particularly suited to fulfill the current standard production process of multi-layered sandwiches, and also to drastically limit the detachment of layers in sandwiches.

The Oberst beam test is a standard method to determine the elastic modulus and the loss factor of a damping material on the basis the frequency response of a multi-layered clamped-free beam (standardized by [4] and [8]). A summary of the procedure and some comments are given in this section, and the relevant expressions are reported in Appendix A.

A base beam of given dimensions (Table 1) and weight is vibrated by a non-contact exciter (Figure 2) and the measured frequencies of the first few flexural modes, together with their analytical expression based on the Bernoulli-Euler model, allow to determine its Young's modulus – eq.(A.1). A layer (or two) of damping material is then bonded on the same beam, according to one of the configurations presented in Figure 1. The composite beam is vibrated again, possibly at different temperatures, and from its dimensions, weight, resonant frequencies and damping ratios, the properties of the viscoelastic material (elastic modulus and loss factor) are inferred – eq.(A.2).

The base beam is supposed to be un-damped so that most often it is metallic but, in the present work, a CFRP material has been used as a support for the damping layer. The first aim was to measure the properties of the CFRP sandwich itself, and the second was to bond the damping layer on the same material as in the actual applications, in order to determine its effectiveness in terms of total damping. It is also worth noticing that in the Oberst model, the damping layer is required to be much more flexible than the supporting beam and this is one of the reasons why the damping layer thickness has to be limited.
The important issue of simulating the interfacial behaviour between different layers, which is addressed by a number of papers with both static and dynamic applications, e.g. [9-13], has not been investigated because of three main reasons. First of all, the procedure for manufacturing the composite beams does not require any additional adhesive layer, since the resins of the viscoelastic material and of the carbon fibre pre-preg undergo the same curing cycle and eventually form a unique component. Secondly, the accelerated aging process showed no detachment of the layers, as attested by both a visual check and the measured mechanical parameters, thus confirming the excellent junction of the layers. Finally, the fitting procedure described in Section 3 does not rely on any specific model aimed at describing neither a sandwich beam nor a CFRP material, but only on a generic multi-degree-of-freedom system.

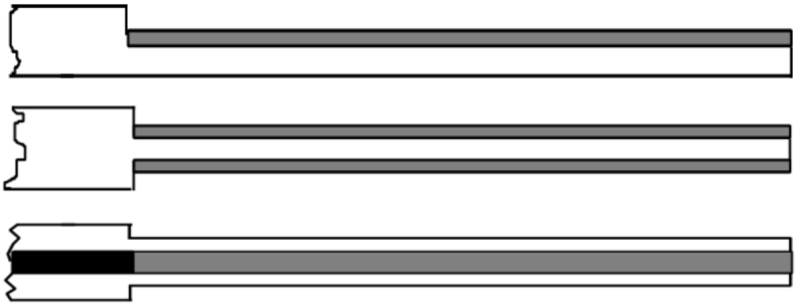

Figure 1 The Oberst beam configurations: single free layer (top), two free layers (centre), constrained layer (bottom). Grey colour indicates the damping material.

The test rig used for the experiments is presented in Figure 2 and Table 1 gives the relevant characteristics of the tested specimens. The free length of the beam was fixed to 200 mm and an electromagnetic contactless exciter MM002 was placed at about 42 mm from the clamping, on the right side in Figure 2, so to avoid the nodes of the first five flexural modes. The magnetic transducer MM0002 is a device produced by Brüel & Kjær and can be used as either a tachometer or an electromagnetic vibration exciter. Both its sensitivity (when used as a velocity sensor) and the applied force (when used as vibration exciter) largely depend on the mean distance from the tested ferromagnetic specimen (the beam in the present case). The producer declares 0.45 N at 0.2 mm and less than 0.15 N at 1.0 mm. The output, proportional to the displacement, has been recorded by a contactless capacitive sensor MM004 placed at the tip of the beam, on the left side in Figure 2. Also this capacitive transducer is produced by Brüel & Kjær and is a displacement sensitive pickup. The distance between the specimen and the transducer is again of great importance because the sensitivity is inversely proportional to the squared distance. The producer declares a typical value of 0.9 V rms with a mean distance of 0.5 mm and a peak-to-peak displacement of 0.1 mm.
It is worth saying that the actual applied force cannot be registered because there is no feedback from the MM0002 device. Nonetheless, the time history of the input force is not really necessary as far as its amplitude is constant in the frequency range of interest (Section 4), which is actually below the 2000 Hz limit reported on the data sheet of the exciter. Also the exact amplitude of motion of the free end of the beam is not strictly necessary. In fact, the fitting procedure presented in Section 3, similarly to the well-established -3dB method, manipulates the frequency response of the beam to extract the natural frequency and damping ratio, whatever the amplitude of oscillation is. In practice, the output voltage of the sensor is directly transformed in the frequency domain, without using the sensor sensitivity.

A swept sine excitation was given in a frequency range covering the flexural natural frequencies two to five because the standards suggest neglecting the first resonance. As regards the number of modes to be analysed, much depends on the distribution and the performances of the damping material. With a proportional damping configuration, as achieved by any of the three arrangements presented in Figure 1, the damping ratio increases with frequency so that high frequency modes usually give rise to a very low amplitude response. As a direct consequence, it is often difficult to obtain reliable results for the damping ratio above the fifth mode of the beam, if the damping material is properly designed. The output (voltage, proportional to displacement) has been recorded by a National Instruments USB-4431 acquisition board, programmed with the dedicated LabView software. The system features a 24 bit δ–σ analogue-to-digital converter, with anti-aliasing filters and adjustable sampling frequency. The sampling frequency was at least four times larger than the fifth resonance frequency and the sweep duration set at five minutes. During this period the compressor and the fan of the climatic chamber (Angelantoni Challenge 250) were switched off so to limit the mechanical noise on the specimen, i.e. to ensure that the only input is due to the magnetic exciter. It is important to keep the sweep duration as long as possible in order to properly excite the specimens, especially in the highly damped sandwich configuration where the response of the beam is limited. On the other hand, the sweep duration has to be as short as possible to maintain a constant temperature within the climatic cell, whose control is switched off during the vibration measurement. Experience indicates that five minutes is a good compromise, producing a temperature variation limited to 1/2 °C and allowing for the application of a satisfactory excitation. Three specimens for each layout have been measured so that the results presented in this paper are to be considered the average values.

Oberst tests have been performed in a thermally controlled environment with temperature rising from -20°C to 60°C, with 10°C steps. The cycle is shown in Figure 3: periods of 1.5 hours at constant temperature were imposed in order to get the thermal equilibrium of the heavy test rig (14.6 kg) and also to complete the temperature progression overnight. The selected range is typical for many different applications, mainly in the automotive sector.

To investigate the aging effect on the behaviour of the materials, the temperature and humidity cycle defined by [14] has been applied (Figure 4). Each specimen has been exposed to the aging cycle for 792 hours, and the Oberst test has been repeated every 264 for a total of four tests for each specimen, simulating environmental exposure effects as reported in [15].

The rationale for selecting the Oberst test is simple: the damping material is in the same configuration (free or constrained layer) as in the actual components (e.g. a door panel) and the same specimen can be repeatedly analyzed. The latter feature not only limits the number of samples to be prepared but also reduces the variability introduced on the results (elastic modulus and loss factor) by the sample characteristics (i.e. slightly changing dimensions and weight), as typical for every non-destructive procedure.

Table 1 Characteristics of the beams (average of three specimens)

Material	Layers (CFRP + damping)	Thickness [mm]	Width [mm]	Length [mm]	Mass [g]	Density [kg/m^3]	Layout
CFRP	3	0,91	12,8	259,9	3,93	1305	Base beam
SUT 9609 One side	3 + 1	1,96	12,8	259,9	8,25	1260	One side
SUT9609 Sandwich	2 + 1 + 2	1,71	12,7	259,8	7,39	1307	Sandwich

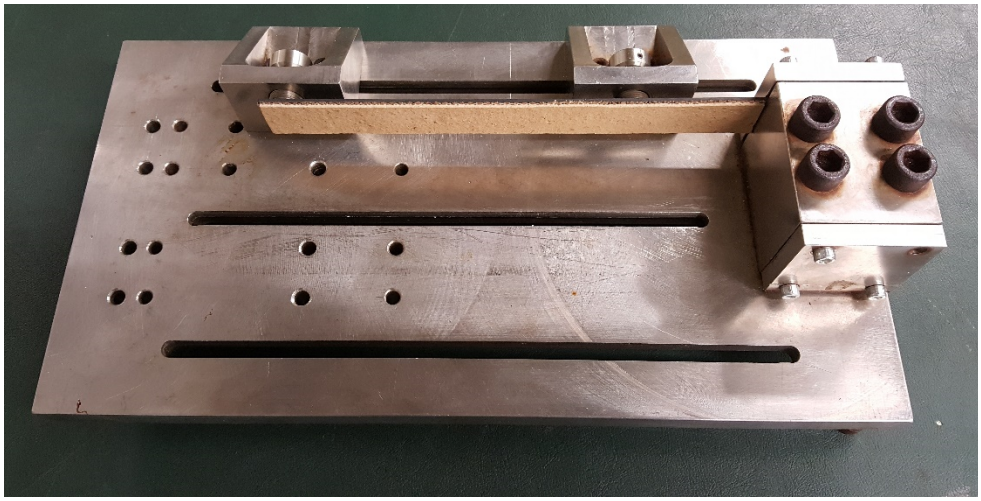

Figure 2 Oberst test bench. Contactless magnetic exciter MM0002 on the right, near the clamping; contactless capacitive displacement sensor MM0004 on the left, near the free end.

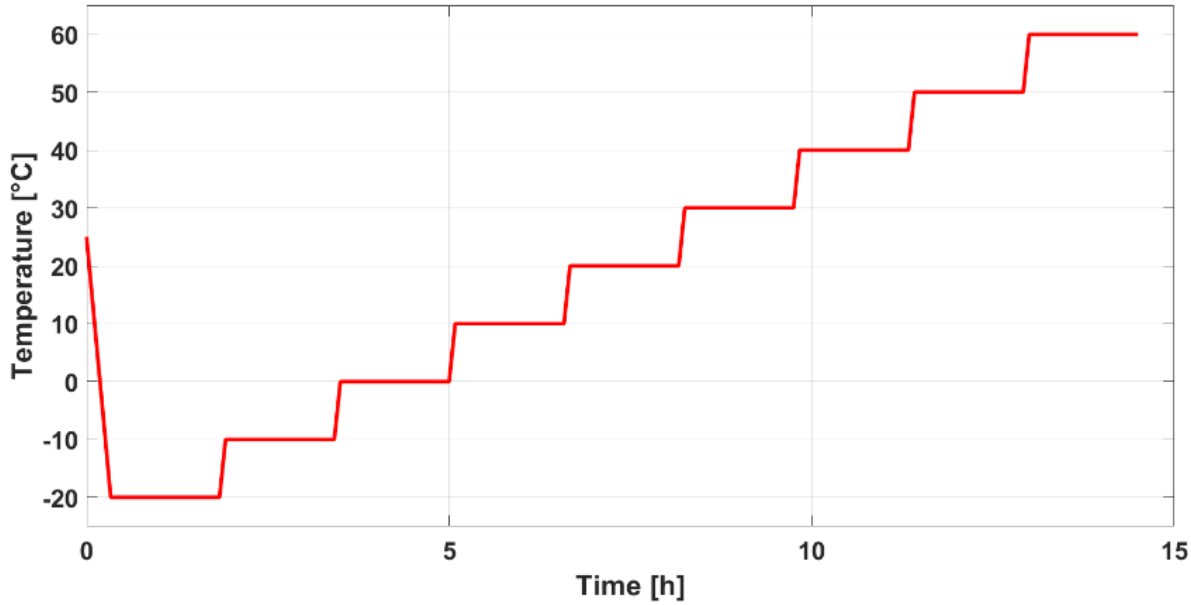

Figure 3 Controlled temperature diagram for the Oberst test. Constant temperature step duration: 1.5 hours.

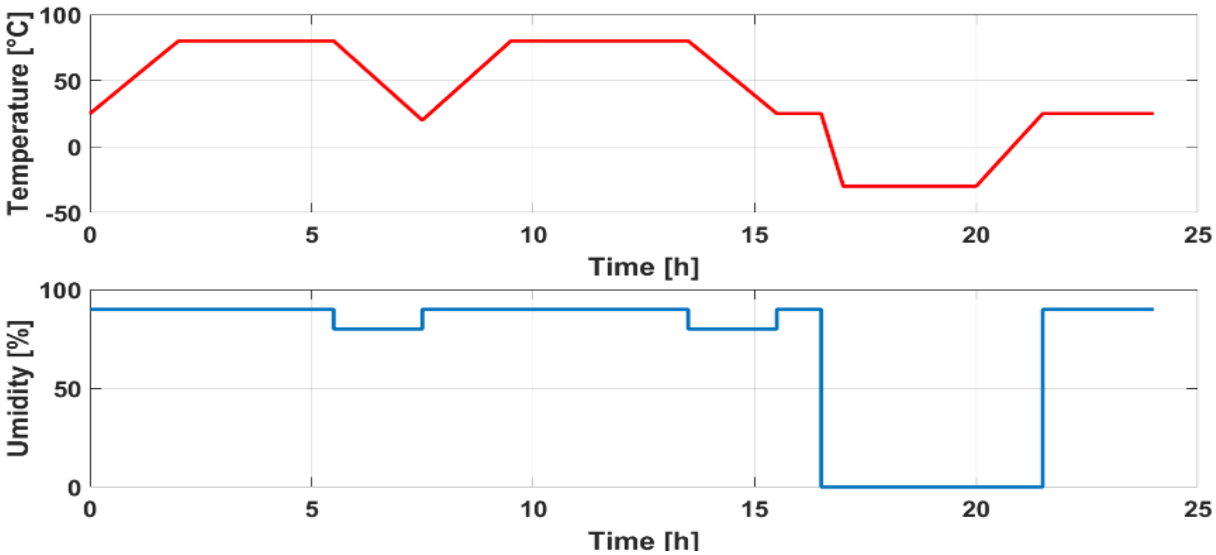

Figure 4 Controlled temperature and humidity diagram for the aging cycle IEC 60068

In brief, the sequence of the testing procedure follows:

a) set the desired temperature and humidity in the environmental test chamber and wait for their stabilisation;
b) switch the chamber off;
c) excite the beam and measure the displacement of its free end. This time domain output is used to compute the PSD S_{yy} (see Section 3.1)
d) switch the chamber on and return to step a).

3 ESTIMATION OF NATURAL FREQUENCY AND DAMPING RATIO

Many standards, e.g. ISO 6721-1 and ASTM E756, suggest relying on the half-power method, also called -3dB method, to determine the natural frequency and damping ratio of a single degree of freedom (SDOF) system. The method requires to plot the resonance curve of the system under forced vibrations and to determine the resonance frequency, which is assumed to be equal to the natural frequency f_n. Two frequencies f_1 and f_2, where the amplitude of the response is 3dB lower than its maximum value, give the width of the resonance peak and then the damping ratio.

$$\zeta = (f_2 - f_1)/(2f_n)$$

It is then usual to link the damping ratio ζ and the loss factor η by the relation $\eta = 2\,\zeta$

The procedure is very simple and very quick to apply but suffers from some drawbacks [16]. In the case of very lightly damped structures, it may be difficult to precisely estimate the value of the maximum amplitude (much depends on the frequency resolution) and, consequently, the values of f_1 and f_2. In the case of very highly damped structures, it may be difficult to get the -3dB points. In any case, only three points of the frequency response are used, although many more spectral lines are usually available. Another very simple and well-known approach is the logarithmic decrement, which is nonetheless limited to the analysis of the free response of single degree of freedom systems [17], which is not the case when a beam is studied.

The method presented in this section is still based on the resonance curve but fits many measured spectral lines (and not only three, f_1, f_2 and f_n) to give a least square evaluation of the natural frequency and the damping ratio. Some numerical examples are presented in Section 3.2 to show the capabilities of the procedure.

The issue of modal parameters identification has indeed interested a large number of scholars both in the linear and non-linear domains [18-21, just to mention a few]. Aim of the following section is to describe a simple method, specifically dedicated to the output-only estimation of frequency and damping ratio.

3.1 THEORY

The impulse response function $h(t)$ of a linear and time invariant system with $\boldsymbol{n}$ degrees of freedom can be expressed in the form

$$h(t) = \sum_{r=1}^{2n} A_r e^{s_r t} \tag{1}$$

and the poles s_r are linked to the natural angular frequencies ω_r and damping ratios ζ_r by the expression $s_r = -\zeta_r\omega_r \pm i\omega_r\sqrt{1-\zeta_r^2}$. The Fourier transform of $h(t)$ gives the frequency response function (FRF) $H(\Omega)$

$$H(\Omega) = \sum_{r=1}^{2n} \frac{A_r}{i\Omega - s_r} \tag{2}$$

The problem is to identify the poles s_r, and then ω_r and ζ_r, given a measured time history $h(t)$ or its correspondent FRF $H(\Omega)$. In the previous expressions (1) and (2), both time and frequency axes are continuous, which is not the case when data are recorded with a digital acquisition system. In practice, a limited (although possibly very large) number of samples is collected in the time domain, which in turn generate a discrete sequence of spectral lines $H_k = H(\Omega_k)$.

Here Ω_k indicates the generic frequency given by

$$\Omega_k = (k-1)\Delta\Omega = (k-1)2\pi\Delta f = \pi f_s(k-1)/(N-1) \tag{3}$$

where f_s is the sampling frequency, Δf is the frequency resolution, N is the number of spectral lines and $k = 1 \ldots N$.
The plot of the modulus of the discrete FRF $|H_k|$, k = 1... N, usually on a logarithmic scale, is the first step for obtaining an estimate of the damping ratio by the half-power method.
The technique described in this section exploits the information of many spectral lines (at least four) around the resonance and takes advantage of expressing the FRF in the *Z*-domain. The *Z* transform of the sampled impulse response function is

$$H_k = \sum_{r=1}^{2n} A_r \frac{z_k}{z_k - z_r} \tag{4}$$

where $z_r = e^{s_r \Delta t}$ and $z_k = e^{i(k-1)\Delta\Omega\Delta t} = e^{i\pi(k-1)(N-1)}$.
z_k indicates the spectral line at frequency Ω_k, z_r is linked to the natural frequency and the damping ratio through s_r, H_k can simply be computed by the fast Fourier transform (FFT). The *Z* transform conveniently maps the frequency axis into a circle, thus limiting to one the modulus of z_k.
If the resonant frequencies are well separated, as also required by the half-power method, a SDOF model can be assumed and Eq. (4) gives, with *n*=1,

$$H_k = \frac{b_1 z_k + b_2 z_k^2}{a_0 + a_1 z_k + z_k^2} \tag{5}$$

where the four unknown coefficients $a_0,\ a_1, b_1,\ b_2$ are real.
The complex z_k can also be written in the form

$$z_k = e^{i\pi(k-1)(N-1)} = e^{ix_k} = \cos x_k + i \sin x_k \tag{6}$$

and then

$$z_k^2 = \cos 2x_k + i \sin 2x_k \tag{7}$$

The squared modulus M_k of the FRF, after the introduction of (6) and (7), into Eq. (5) is

$$M_k = |H_k|^2 = H_k^* H_k = \frac{1 + A\ cosx_k}{B + C\ cosx_k + D \cos 2x_k} \tag{8}$$

where * indicates the complex conjugate. The four real coefficients are given by:

$$A = p/q \qquad B = (1 + a_0^2 + a_1^2)/q \qquad C = 2a_1\ (1 + a_0\ )/q \qquad D = 2a_0\ /q$$
$$p = 2b_1\ b_2 \qquad q = b_1^2 + b_2^2.$$

It is important to notice that in the Oberst beam test the FRF is not available since the input is applied by a contactless exciter and cannot be measured. But, under the usual assumption that the power spectral density (PSD) of the input is flat in the frequency range of interest (which is the case also for the half-power method), the PSD S_{yy} of the measured output is proportional to the squared modulus M_k of the FRF, i.e. $S_{yy}(\Omega_k) \propto M_k \equiv |H_k|^2$. In this case, for every spectral line *k*, i.e. at every frequency Ω_k, it is then possible to arrange eq. (8) in the form

$$-\cos x_k\ \mathrm{A} + M_k\ \mathrm{B} + M_k \cos x_k\ \mathrm{C} + M_k \cos 2x_k\ \mathrm{D} = 1 \tag{9}$$

which leads to the following linear system of equations

$$\begin{bmatrix} -\cos x_p & M_p & M_p \cos x_p & M_p \cos 2x_p \\ -\cos x_{p+1} & M_{p+1} & M_{p+1} \cos x_{p+1} & M_{p+1} \cos 2x_{p+1} \\ \vdots & \vdots & \vdots & \vdots \\ -\cos x_q & M_q & M_q \cos x_q & M_q \cos 2x_q \end{bmatrix} \begin{Bmatrix} \mathrm{A} \\ \mathrm{B} \\ \mathrm{C} \\ \mathrm{D} \end{Bmatrix} = \begin{Bmatrix} 1 \\ 1 \\ 1 \\ 1 \end{Bmatrix} \tag{10}$$

p and q respectively indicate the lowest and highest frequencies of interest around the resonance and K=q-p+1 is the number of spectral lines. When K>4, eq.(10) is an overdetermined system of equations that can be solved in a least square sense, for example with a singular value decomposition.
With A, B, C and D it is then possible to determine a_0 and a_1 and finally, since $a_0 = z_r\ z_r^*$ and $a_1 = z_r\ + z_r^*$, to retrieve the natural frequency ω_r and damping ratio ζ_r:

$$\omega_r = \sqrt{\left[f_s \operatorname{acos}\left(-\frac{1}{2}\frac{a_1}{\sqrt{a_0}}\right)\right]^2 + \left(\frac{f_s}{2} \ln a_0\right)^2} \tag{11}$$

$$\zeta_r = \left(-\frac{f_s}{2} \ln a_0\right)/\omega_r \tag{12}$$

The proposed method is not as easy as the half-power technique but offers at least three advantages:

1) it is based on many spectral lines and gives a least square solution for both ω_r and ζ_r;
2) it can be applied also to highly damped structures;
3) a synthesized PSD –based on Eq. (8) – can be plotted to visually verify if it correctly fits the original data

An open source Matlab® implementation of the fitting procedure can be obtained from the authors under the CC-by license.

3.2 NUMERICAL EXAMPLES

The first two examples use a single degree of freedom system with natural frequency 1 Hz and damping ratio either very small (0.2 %) or very large (40%). Every spectral line of the theoretical FRF of the model has been numerically corrupted with 3% random noise to simulate possible inaccuracies in the measuring apparatus. The resulting PSDs are presented in Figure 5 and Figure 6. In both cases the application of the 3dB method would be very difficult: with ζ=0.02%, the estimation of both the maximum amplitude and the width of the resonance peak can be largely inaccurate (in fact the spectral line at 1 Hz is not present); with ζ=40%, the half power points are hard to find and it is not possible to assume that the natural (1 Hz) and resonance (about 0.8 Hz) frequencies are numerically equivalent.

The results of the fitting procedure are graphically represented in Figure 7 and Figure 8 where the original spectra, black solid lines with black dots, are overlaid on the synthesized curves (red dashed lines). The representation of the synthesized PSD gives also a qualitative estimation of the numerical results, which are indeed very satisfactory: 0.19% and 40.1%. When the peak is very sharp, i.e. the damping ratio is very small, a few spectral lines (less than ten in Figure 7) are sufficient to obtain accurate results, while larger values of damping require more spectral lines (about 100 in Figure 8). It is possible to conclude that the method is robust and can cope also with noisy data, as far as a SDOF system is concerned.

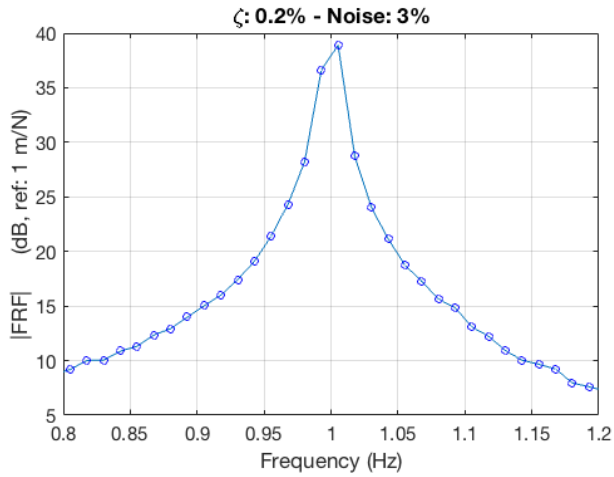

Figure 5 modulus of the FRF of a SDOF system with very small (0.2%) damping ratio

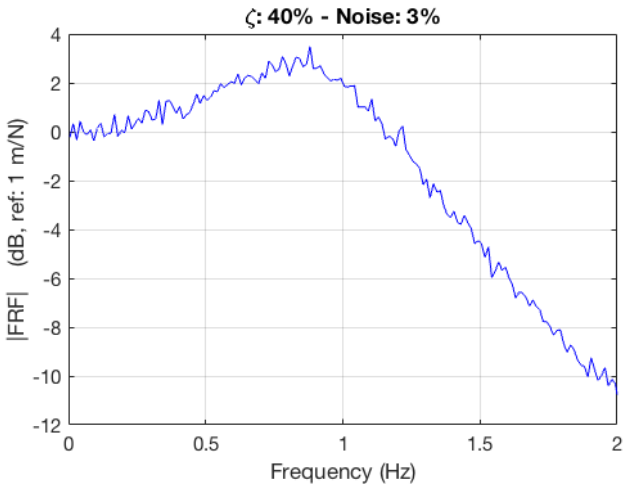

Figure 6 modulus of the FRF of a SDOF system with very high (40%) damping ratio

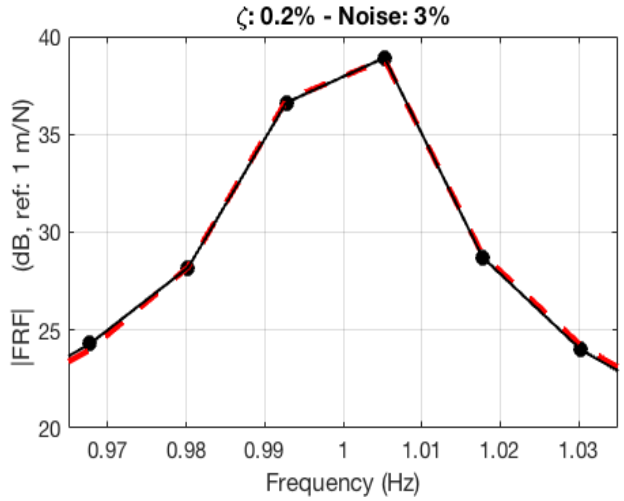

Figure 7 results of the fitting procedure with very small (0.2%) damping ratio. Red dashed line: synthesized curve; black solid line with dots: original data.

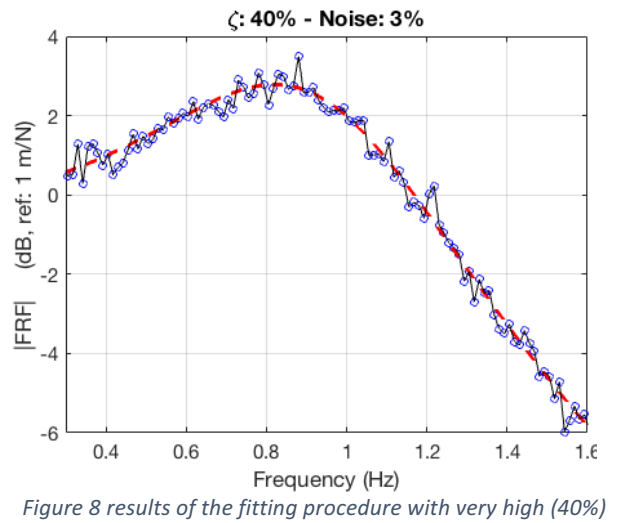

Figure 8 results of the fitting procedure with very high (40%) damping ratio. Red dashed line: synthetized curve; black solid line with dots: original data.

In order to verify the effectiveness of the fitting procedure with a multi-degree of freedom (MDOF) system, a finite element model (FEM) of the Oberst beam has been prepared with dimensions 200x20x0.9 mm^3 (length/width/thickness), in a clamped-free configuration. Convergence tests on the eigenvalues of the FEM suggested that a 100/10 mesh with shell elements (1000 in total) is appropriate to achieve correct results.
Damping has been introduced according to the viscous proportional model

$$[C] = \alpha[M] + \beta[K] \tag{13}$$

so that various levels of dissipation can simply be obtained just by changing α and β.
The FRF has been computed between FE nodes located in positions similar to the input and output points of the actual test rig. The selected output node is not in the exact midline of the model, so to simulate a possible defect in the output sensor position, and consequently also the unwanted contribution of the torsional modes will be present in the FRF.
Two examples with very small and very high damping ratios are proposed, and again with 3% noise on each spectral line. Also in this case the application of the -3dB method would be complicated by either too low or too high damping ratios and this is the reason why a direct comparison with the -3dB method is not reported.
In Table 2, the method is instead validated by comparison with the theoretical results. The first flexural mode (Figure 9, 17.1 Hz) is neglected, as suggested by the standard, as well as the torsional modes at about 170 and 500 Hz. In the low damping case, the fifth damping ratio is underestimated, both because of the noise introduced in the spectrum and the influence of non-resonant modes. Also the first estimation is lower than expected but its value is so low (0.2 %) that the difference is negligible. When the high damping case is studied (Figure 9) Mode 4 at about 600 Hz is almost undetectable and largely modified by the other modes. The resulting fitting curve (Figure 10) is not very accurate because a SDOF model cannot correctly describe the shape of the MDOF system, and also because of the noise. Consequently, both frequency and damping estimations are far from the correct values. This conclusion is not unexpected, as also reported by [16]. Moreover, Mode 5 completely disappears from the resulting output (a resonance peak in the FRF cannot even be spotted) and cannot be detected, but the estimates of Mode 2 (110 Hz) and Mode 3 (310 Hz) are still very accurate.

The numerical results suggest that:

- the proposed method is applicable to both high and low damped resonance curves;
- the least square solution can limit the influence of noise to a great extent;
- the SDOF approximation is not too restrictive, provided that modes are well separated;
- the synthesized PSD is a simple but effective tool to judge the quality of the results.

Of course the solution of Eq. (10) is more complicated than computing the ratio $\eta = (f_2 - f_1)/f_n$. But, given a proper software, the end user just has to choose p and q in eq.(10) to achieve reliable results.

Table 2 estimated damping ratios and frequencies from the FE beam model. Two cases: low and high damping

		Mode 2	Mode 3	Mode 4	Mode 5
			Damping ratio	(%)	
Low damping	Theoretical	0.21	0.59	1.1	1.9
	Extracted	0.17	0.57	1.1	1.7
High damping	Theoretical	2.1	5.9	11.5	17.0
	Extracted	2.1	5.9	16.8	---
			Frequency	(Hz)	
Low damping	Theoretical	110.8	310.3	608.2	1005
	Extracted	110.7	311.1	610.1	1008
High damping	Theoretical	110.8	310.3	608.2	1005
	Extracted	111.8	306.8	620	---

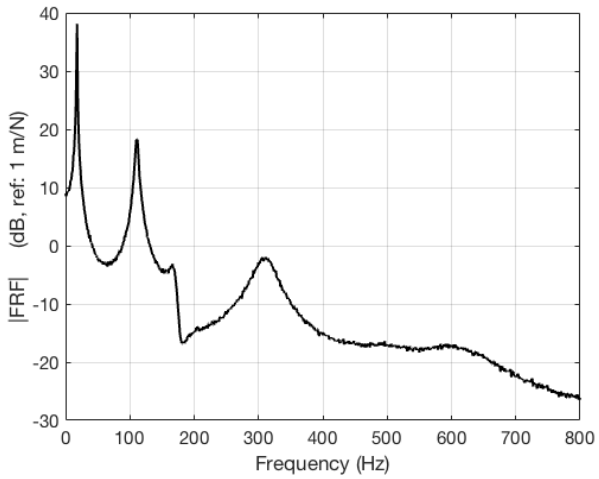

Figure 9 modulus of the output of the FEM beam in the high damping case

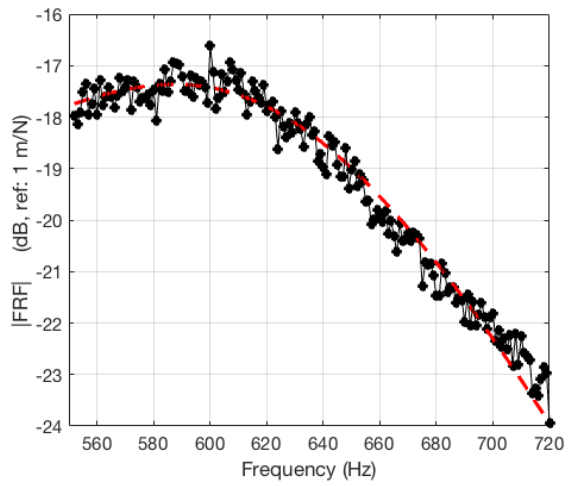

Figure 10 fitting of the 4th flexural mode, high damping case. Red dashed line: synthesized curve; black solid line with dots: original data

4 EXPERIMENTAL RESULTS

This section presents the results obtained by analyzing the beams listed in Figure 1. All the values are the average over three samples of the same type.

4.1 BASE BEAM

The base beam has been named "T300" because it is formed by three layers of T300 (twill 200 gr/m^2) carbon fabric in an epoxy matrix. The three samples under investigation have been cut from the same plate so that they underwent the same production process.

Figure 11 shows Young's modulus and loss factor of T300 beam, as a function of temperature. The reported values, almost perfectly constant, are obtained as an average over modes from two to five. The loss factor is almost null and completely comparable with the values collected from a steel beam 1 mm thick, thus confirming the possibility of using T300 as a base beam for the damping materials. The aging cycle, at least up to 792 hours, does not notably modify the material. Not only the external aspect does not change, but also the mechanical properties are invariant with only a slight increment of the elastic modulus.

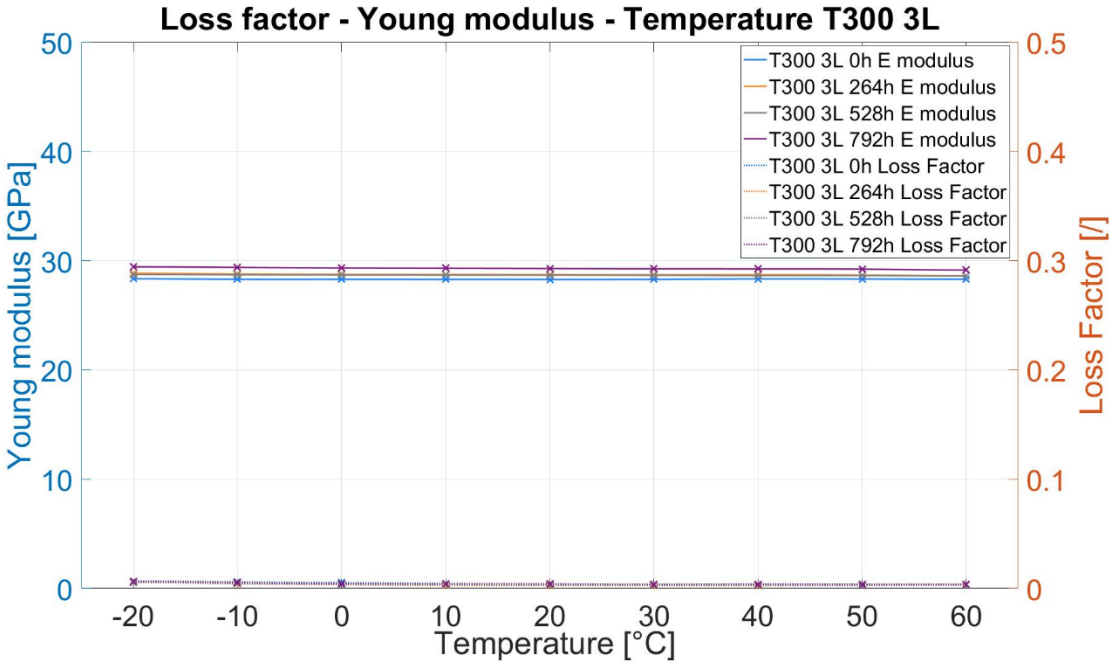

Figure 11 T300 loss factor and Young's modulus as function of temperature and aging condition

4.2 DAMPING MATERIAL PROPERTIES

Figure 12 presents the elastic modulus of the damping material, as deduced by applying the ASTM expressions (Appendix A) to the experimental results of three beams damped on a single side (see Figure 1). At -10°C two points only are plotted because at that temperature only modes two and three can correctly be fitted, due to the high level of dissipation introduced by the damping material. The figure makes it clear that large variations occur in the selected temperature range -20/60 °C while frequency, although not completely negligible, only exerts a low influence on the material in the 100-800 Hz range.

Since the frequency variations are not so pronounced, and taking into account that in any actual installation the damping material is likely to be excited and to respond in a large frequency band, it has been decided to group the results. Figure 13 gives Young's modulus and loss factor of the damping material (KRAIBON® SUT9609), calculated as the mean value of many modes, from two to four depending on temperature. At each temperature the scatter about the mean is also plotted, for the four curves representing the aging progression. The loss factor largely depends on temperature, with some variance due to frequency, but exhibits almost no dependency on the aging cycles although in this configuration (one side damping) the damping layer is directly exposed to humidity and ice.

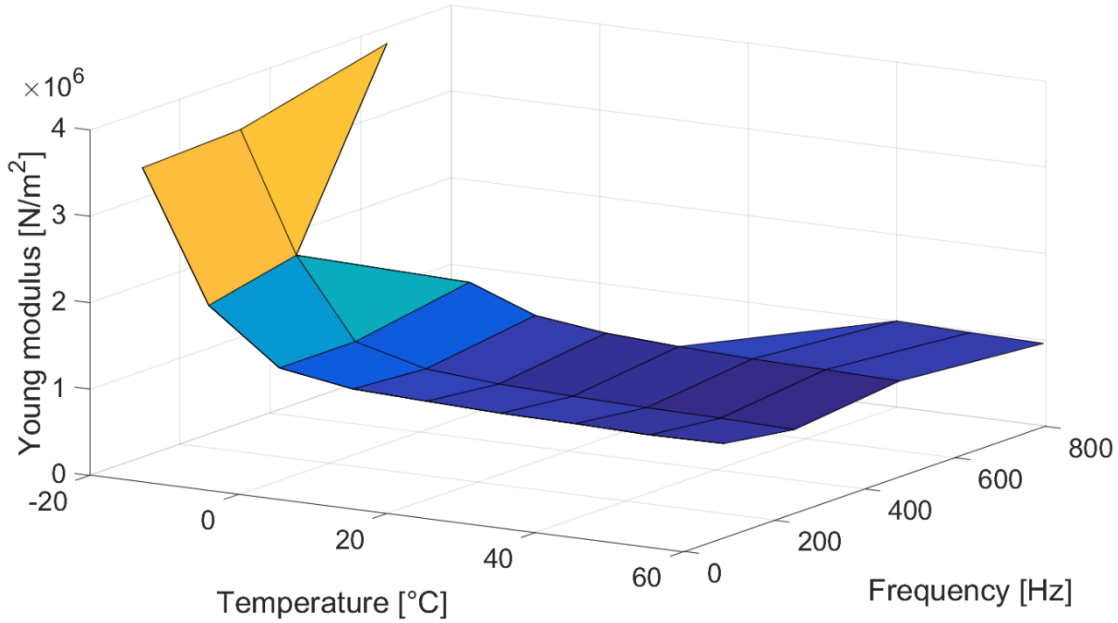

Figure 12 Young's modulus of the damping material, estimated according to ASTM (beam damped on one side, Appendix A) before the aging process.

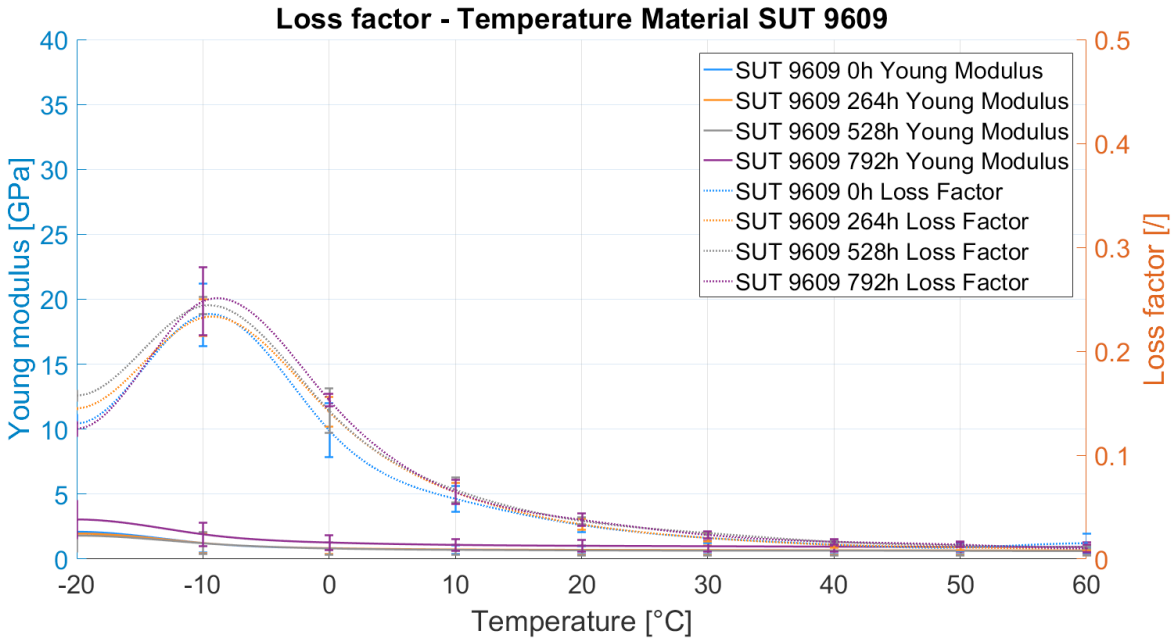

Figure 13 Pure material, loss factor and Young's modulus (with their dispersion bars) as function of temperature and aging conditions

4.3 SANDWICH BEAM vs ONE SIDE DAMPED BEAM

The last example underlines the different effects that can be obtained by using the free (beam damped on one side) and constrained (sandwich beam) damping layer configurations. Figure 14 and Figure 15 display the elastic modulus and the loss factor of two composites: the beam damped on one side (free damping layer) and the sandwich beam (constrained damping layer), as per Figure 1. In this case, the specimens have been studied as if they were formed by a single homogeneous material and the plotted loss factors then have the effective values assumed by the specimens themselves.
The influence of the stacking sequence (free or constrained layer) is of paramount importance in modifying the results: the damping properties of the sandwich beam not only are larger but also span

a wider temperature range in comparison with the free layer configuration. The results presented in this section show that temperature largely modifies the behaviour of the composite and that, apart from the *0 h* aging condition in the sandwich beam, the accelerated aging cycle does not evidently affect the properties of the tested specimen, at least up to 792 hours. Table 3 lists Young's modulus and loss factor of both beams, given as the mean value of four (0-264-528-792 hours; free layer) and three (264-528-792 hours; constrained layer) aging steps.

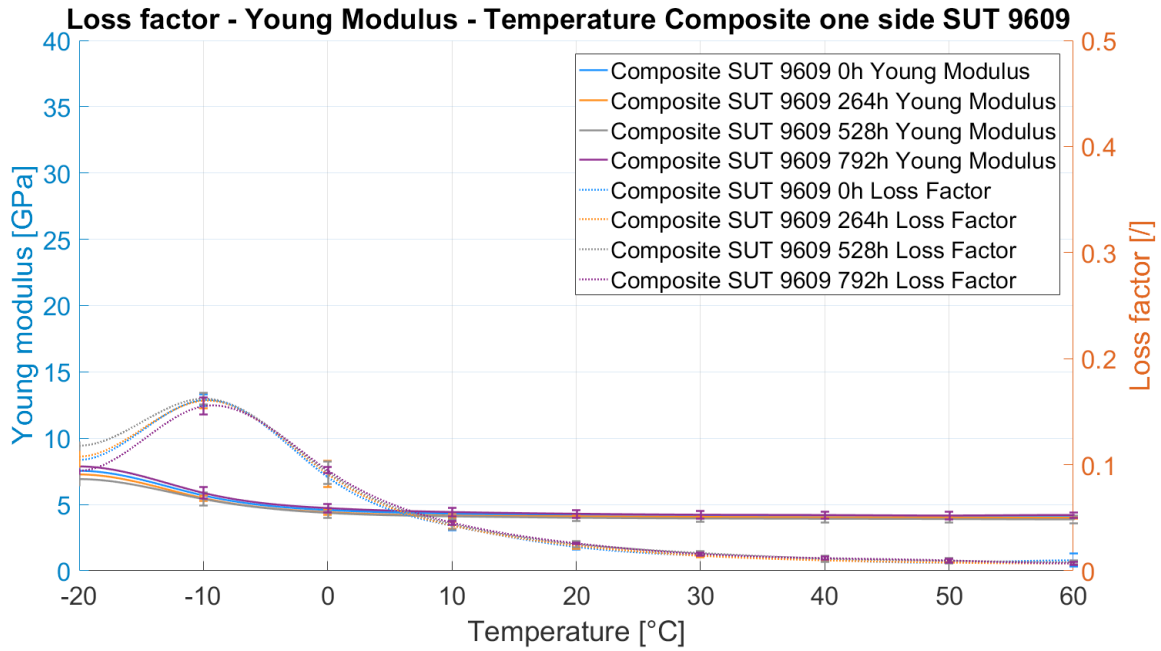

Figure 14 Beam damped on one side, loss factor and Young's modulus (with their dispersion bars) as a function of temperature and aging conditions

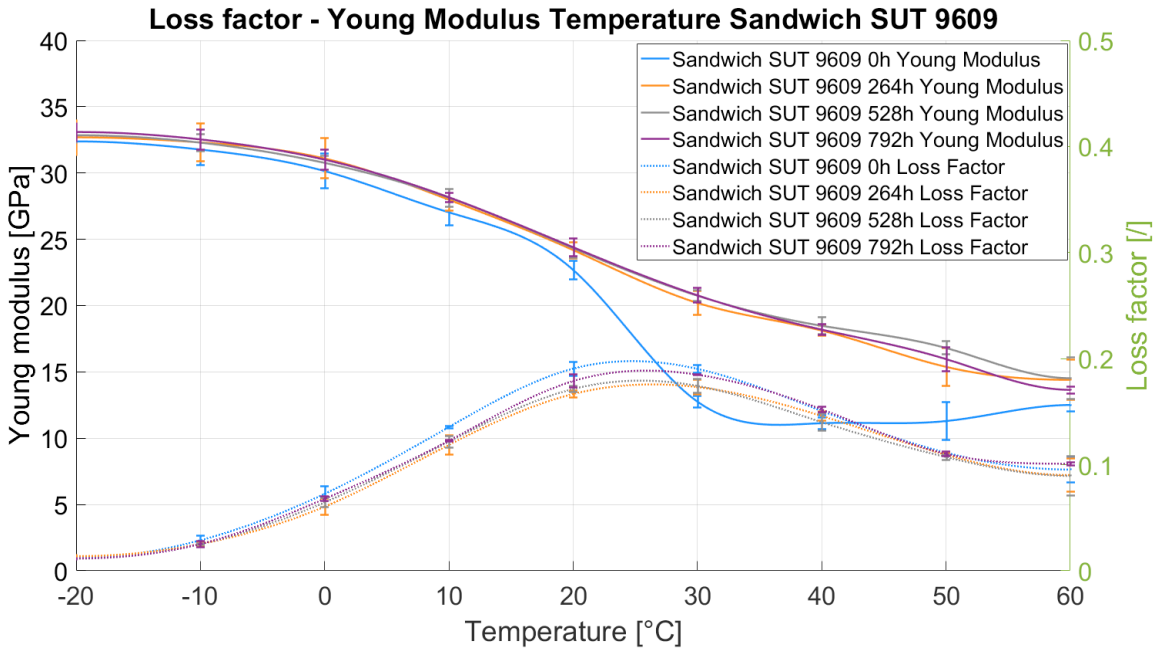

Figure 15 Sandwich beam, loss factor and Young's modulus (with their dispersion bars) as a function of temperature and aging condition

Table 3 Mean values of Young's modulus and loss factor. Two cases: beam damped one side and sandwich beam

Beam damped one side									
T [°C]	*-20*	*-10*	*0*	*10*	*20*	*30*	*40*	*50*	*60*
E [GPa]	7,40	5,61	4,52	4,25	4,15	4,10	4,07	4,05	4,04
η [%]	10,61%	15,97%	9,17%	4,36%	2,43%	1,53%	1,08%	0,86%	0,80%
Sandwich beam									
T [°C]	*-20*	*-10*	*0*	*10*	*20*	*30*	*40*	*50*	*60*
E [GPa]	32,91	32,40	30,95	28,07	24,25	20,56	18,40	16,05	13,96
η [%]	1,23%	2,52%	6,43%	12,10%	17,23%	17,74%	14,61%	10,90%	9,35%

5 CONCLUSIONS

Vehicles electrification and new targets concerning the fuel consumption impose a continuous research in weight reduction. Consequently, the use composite lightweight material with efficient mechanical characteristics will play a central role in future vehicle components. For this reason, the material used as a baseline for the research is a CFRP.

The paper presents an accurate least squares fitting method to evaluate the natural frequency and the loss factor of a SDOF system from experimental data. The response is analyzed in the frequency range containing the resonance of the system and since the method relies on a large number of spectral lines, the limitations of the classical half-power points method are eliminated. Numerical examples show that the procedure is very accurate also for MDOFs systems, as far as the modes are uncoupled, and has successfully been applied to the analysis of the Oberst beam test recordings.

Experimentation confirmed that the Oberst test is a reliable, fast and non-destructive procedure which permits a definition of materials database characteristics, that can be incorporated in FE analyses as done in [22, 23]. The chosen damping material can very simply be added in the production process of any CFRP sandwich: it can be handled just like any other carbon fiber layer, it does not require the use of any specific tools and can be subjected to the same curing process of the epoxy resins. Experimentally obtained data have been averaged over three specimens and, although the number of samples is too low to allow for a correct statistical analysis, the scatter of the results from the mean value remains under 3% for each material. Each material has been tested in the -20/+60 °C temperature range, which is in line with SAE specifications for automotive components and proved to encompass the temperature of maximum damping effectiveness. The adopted aging cycle, combining the effects of temperature and humidity, did not yield any significant effect on the materials characteristics, neither on the external aspect nor on their mechanical properties. The only difference is showed by the first aging step of sandwich samples, which displays an altered behaviour from 20°C to 60°C.

In summary, this paper presents a new fitting procedure that efficiently allows to determine the natural frequency and the damping ratio of an output-only frequency response function. These quantities, combined with the model of the Oberst beam test, yield the elastic modulus and the loss factor of the specimen. A particular damping material, whose formulation permits a simple inclusion in the stacking sequence of a common CFRP sandwich, has then been characterized as a function of both frequency and temperature. The stability of its mechanical properties during an accelerated aging cycle has finally been verified.

Acknowledgments

The authors wish to acknowledge: Altair-Italy Engineering S.R.L. for providing the FE software and Gummiwerk KRAIBURG GmbH for the damping material "KRAIBON® SUT9609/24" and the active support during all the activity and G. Angeloni® S.R.L. for the structural CFRP material.

BIBLIOGRAPHY

[1] K. Govindswamy, T. Wellmann, and G. Eisele, “Aspects of NVH Integration in Hybrid Vehicles,” *SAE Int. J. Passeng. Cars - Mech. Syst.*, vol. 2, no. 1, pp. 1396–1405, May 2009.

[2] G. Eisele, K. Wolff, M. Wittler, R. Abtahi, and S. Pischinger, “NVH of Hybrid Vehicles.”, 1: FEV Motorentechnik GmbH, Neuenhofsteaβe 181, 52078 Aachen, Germany, 2: Institute for Combustion Engines of RWTH Aachen University; Schinkelstraβe 8, 52062 Aachen Germany, pp 39 - 44 2010.

[3] K.-W. Kim *et al.*, “Cure behaviors and mechanical properties of carbon fiber-reinforced nylon6/epoxy blended matrix composites,” *Compos. Part B Eng.*, vol. 112, pp. 15–21, Mar. 2017.

[4] American Society for Testing and Materials International, *ASTM E756 – 05 (Reapproved 2010). Standard Test Method for Measuring Vibration-Damping Properties of Materials*. 2010.

[5] M. Fagone, F. Loccarini, and G. Ranocchiai, “Strength evaluation of jute fabric for the reinforcement of rammed earth structures,” *Compos. Part B Eng.*, vol. 113, pp. 1–13, Mar. 2017.

[6] M. Mastali, A. Dalvand, and A. Sattarifard, “The impact resistance and mechanical properties of the reinforced self-compacting concrete incorporating recycled CFRP fiber with different lengths and dosages,” *Compos. Part B Eng.*, vol. 112, pp. 74–92, Mar. 2017.

[7] M. A. Al-Zubi, E. O. Ayorinde, M. A. Dundar, M. Warriach, and Y. Murty, “Vibro-Acoustic Characterization and Optimization of Periodic Cellular Material Structures (PCMS) for NVH Applications,” *J. Mater. Sci. Res.*, vol. 2, no. 4, Sep. 2013.

[8] *SAE J1637 (1993). Laboratory measurement of the composite vibration damping properties of materials on a supporting steel bar*, vol. SAE International. 1993.

[9] J. M. Bai , and C. T. Sun, "The Effect of Viscoelastic Adhesive Layers on Structural Damping of Sandwich Beams", Mechanics of Structures and Machines, vol. 23, Issue 1, pp. 1-16, 1995

[10] S. Yang, R.F. Gibson, L. Gu, and W.-H. Chen, "Modal parameter evaluation of degraded adhesively bonded composite beams", Composite structures, vol. 43, issue 1, pp. 79-91, 1998

[11] C. Jin, and X. Wang, " The effect of adhesive layers on the dynamic behavior of surface-bonded piezoelectric sensors with debonding", Journal of Intelligent Material Systems and Structures, vol. 22, Issue 7, pp. 615-629, 2011.

[12] F. Ascione, G. Mancusi, S. Spadea, M. Lamberti, F. Lebon, and A. Maurel-Pantel, "On the flexural behaviour of GFRP beams obtained by bonding simple panels: An experimental investigation", Composite Structures, vol. 131, pp. 55-65, 2017.

[13] V. N. Burlayenko, and T. Sadowski, "Influence of skin/core debonding on free vibration behavior of foam and honeycomb cored sandwich plates", International Journal of Non-Linear Mechanics, vol. 45, Issue 10, pp.959-968, 2010

[14] IEC 60068 - 2 - 1 International Electrotechnical Commission, International standard for Environmental testing.

[15] A. Nobili and C. Signorini, “On the effect of curing time and environmental exposure on impregnated Carbon Fabric Reinforced Cementitious Matrix (CFRCM) composite with design considerations,” *Compos. Part B Eng.*, vol. 112, pp. 300–313, Mar. 2017.

[16] G. A. Papagiannopoulos and G. D. Hatzigeorgiou, “On the use of the half-power bandwidth method to estimate damping in building structures,” *Soil Dyn. Earthq. Eng.*, vol. 31, no. 7, pp. 1075–1079, Jul. 2011.

[17] D. J. Tweten, Z. Ballard, and B. P. Mann, “Minimizing error in the logarithmic decrement method through uncertainty propagation”, Journal of Sound and Vibration, vol. 333(13), pp. 2804-2811, 2014.

[18] Sadhu, S. Narasimhan, J. Antoni, “A review of output-only structural mode identification literature employing blind source separation methods”, Mechanical Systems and Signal Processing, vol. 94, pp. 415-431, Sept. 2017.
[19] N. Maia, J. Silva, Theoretical and experimental modal analysis, John Wiley and Sons, New York, 1997.
[20] E. Gandino, L. Garibaldi, S. Marchesiello, “Covariance-driven subspace identification: A complete input–output approach”, Journal of Sound and Vibration, vol. 332, no. 26, pp. 7000-7017, 2013.
[21] G. Kerschen, M. Peeters, J.C. Golinval, C. Stéphan, “Nonlinear Modal Analysis of a Full-Scale Aircraft”, Journal of Aircraft, American Institute of Aeronautics and Astronautics, vol 50 (5), pp. 1409-1419, 2013.
[22] J. Pach, D. Pyka, K. Jamroziak, and P. Mayer, “The experimental and numerical analysis of the ballistic resistance of polymer composites,” *Compos. Part B Eng.*, vol. 113, pp. 24–30, Mar. 2017.
[23] A. Fasana, M. Carello, A. Ferraris, A. Airale, and D. B. Polato, “NVH Analysis of Automotive Components: A Carbon Fiber Suspension System Case,” in *Advances in Italian Mechanism Science*, vol. 47, G. Boschetti and A. Gasparetto, Eds. Cham: Springer International Publishing, 2017, pp. 345–354.

APPENDIX A

Structural base beam:

$$E = \frac{(12\rho l^4 f_n^2)}{(H^2 C_n^2)}$$

$$\eta = \frac{(\Delta f_n)}{(f_n)}$$

Where:

C_n *= coefficient for mode n of clamped-free (uniform) beam,*
E = Young's modulus of beam material, Pa,
fn = the resonance frequency for mode n, Hz,
Δf_n *= the half-power bandwidth of mode n, Hz,*
H = thickness of beam in vibration direction, m,
l = length of beam, m,
n = mode number: 1, 2, 3. . .
η *= loss factor of beam material, dimensionless,*
ρ *= density of beam, kg/m3,*
C1 = 0,55959,
C2 = 3,5069,
C3 = 9,8194,
C4 = 19,242,
C5 = 31,809,
$C_n = \left(\frac{\pi}{2}\right)(n - 0{,}5)^2$ *for n>3.*

Beam damped on one side:

$$E_1 = \frac{E}{(2T^3)}\left[(\alpha - \beta) + \sqrt{\{(\alpha - \beta)^2 - 4T^2(1 - \alpha)\}}\right]$$

$$\eta_1 = \eta_c\left[\frac{(1 + MT)(1 + 4MT + 6MT^2 + 4MT^3 + M^2T^4)}{(MT)(3 + 6T + 4T^2 + 2MT^3 + M^2T^4)}\right]$$

Where:
D= ρ1/ρ density ratio,
E = Young's modulus of beam material, Pa,
E1 = Young's modulus of damping material, Pa,
fn = the resonance frequency for mode n, Hz,
fc = the resonance frequency for mode c of composite beam, Hz,
Δf_c *= the half-power bandwidth of mode c of composite beam, Hz,*
H = thickness of base beam, m,
H1 = thickness of damping material, m,
M = E1/E Young modulus ratio,
T = H1 /H thickness ratio,
$\alpha = \left(\frac{f_c}{f_n}\right)^2 (1 + DT)$,
β *= 4+6T+4T2,*
c = index number: 1, 2, 3 . . . c=n,
ηc *= loss factor of composite beam, dimensionless,*
$\eta 1$ *= loss factor of damping material, dimensionless,*
ρ *= density of base beam, kg/m3,*
$\rho 1$ *= density of damping material, kg/m3.*